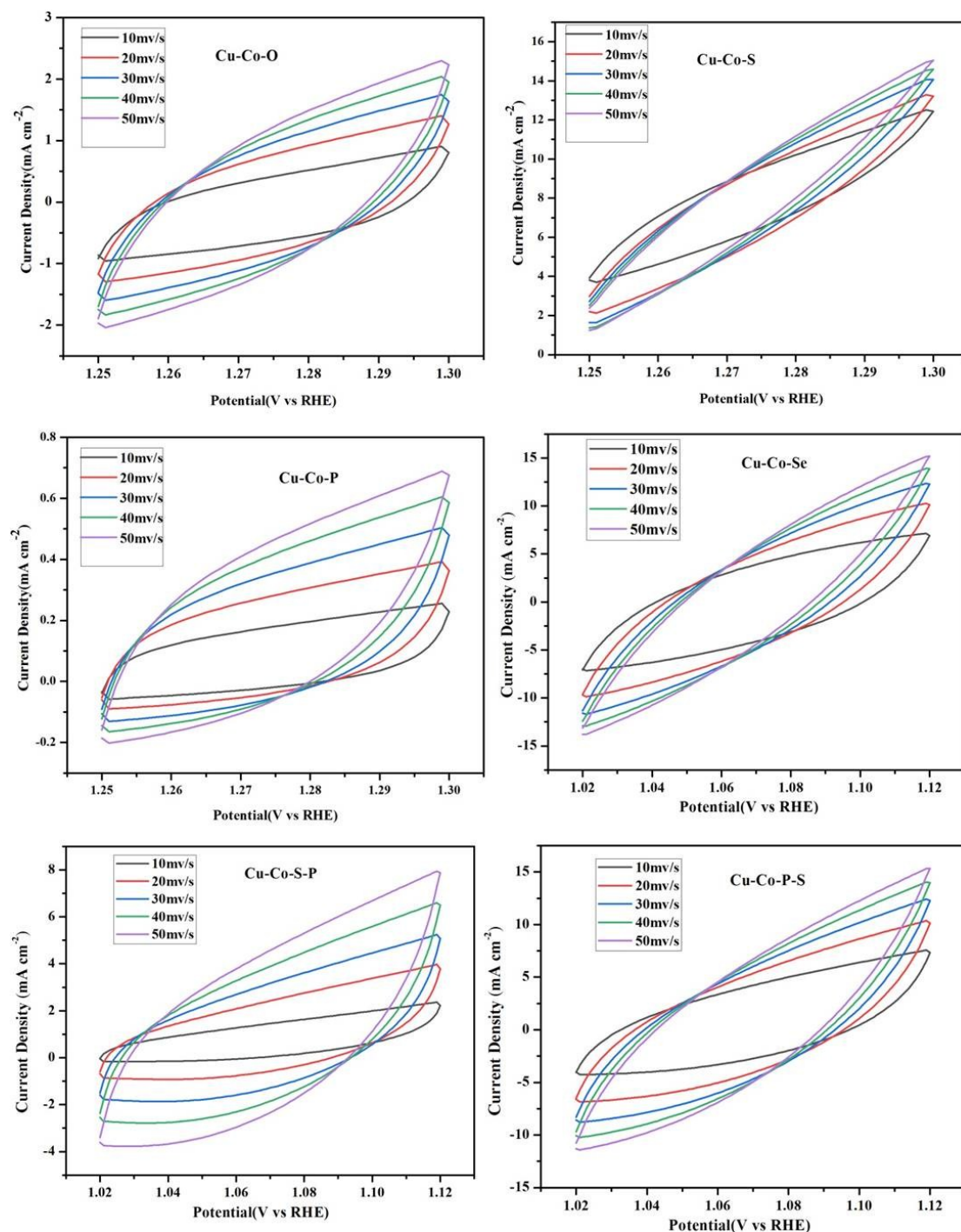
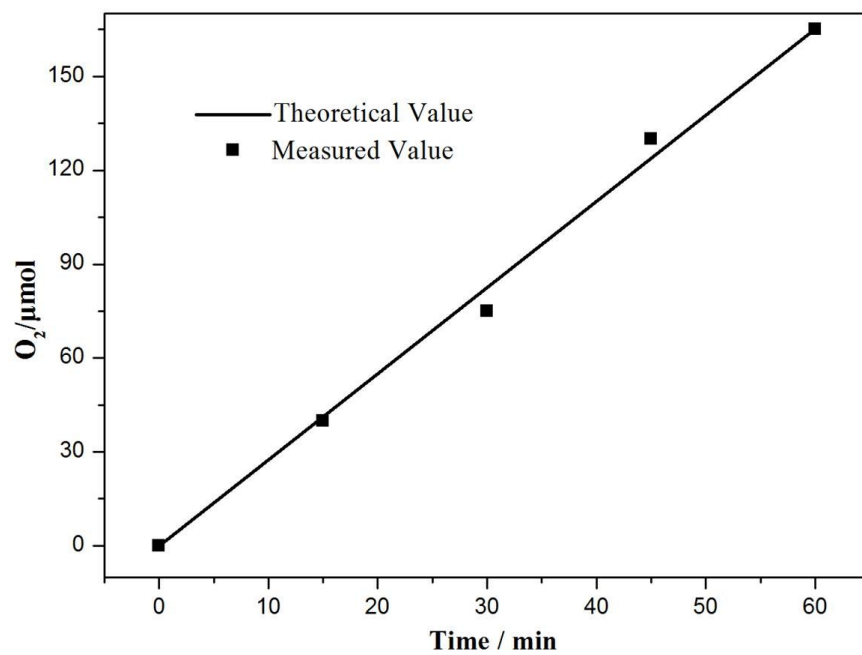


## Cu-Co-M arrays on Ni foam as monolithic structured catalysts for water splitting: effects of co-doped S-P

Xiaoqiang Du<sup>a\*</sup>, Qizhao Shao<sup>a</sup> and Xiaoshuang Zhang<sup>b\*</sup>



**Fig. S1** CVs of Cu-Co-O, Cu-Co-S, Cu-Co-P, Cu-Co-Se, Cu-Co-S-P and Cu-Co-P-S with different scan rates (10-50 mV s<sup>-1</sup>) in the region of 1.02-1.12V vs RHE.



**Fig. S2** Electrocatalytic efficiency of  $O_2$  production over Cu-Co-P-S at a potential of ca. 1.50 V, measured for 60 min.

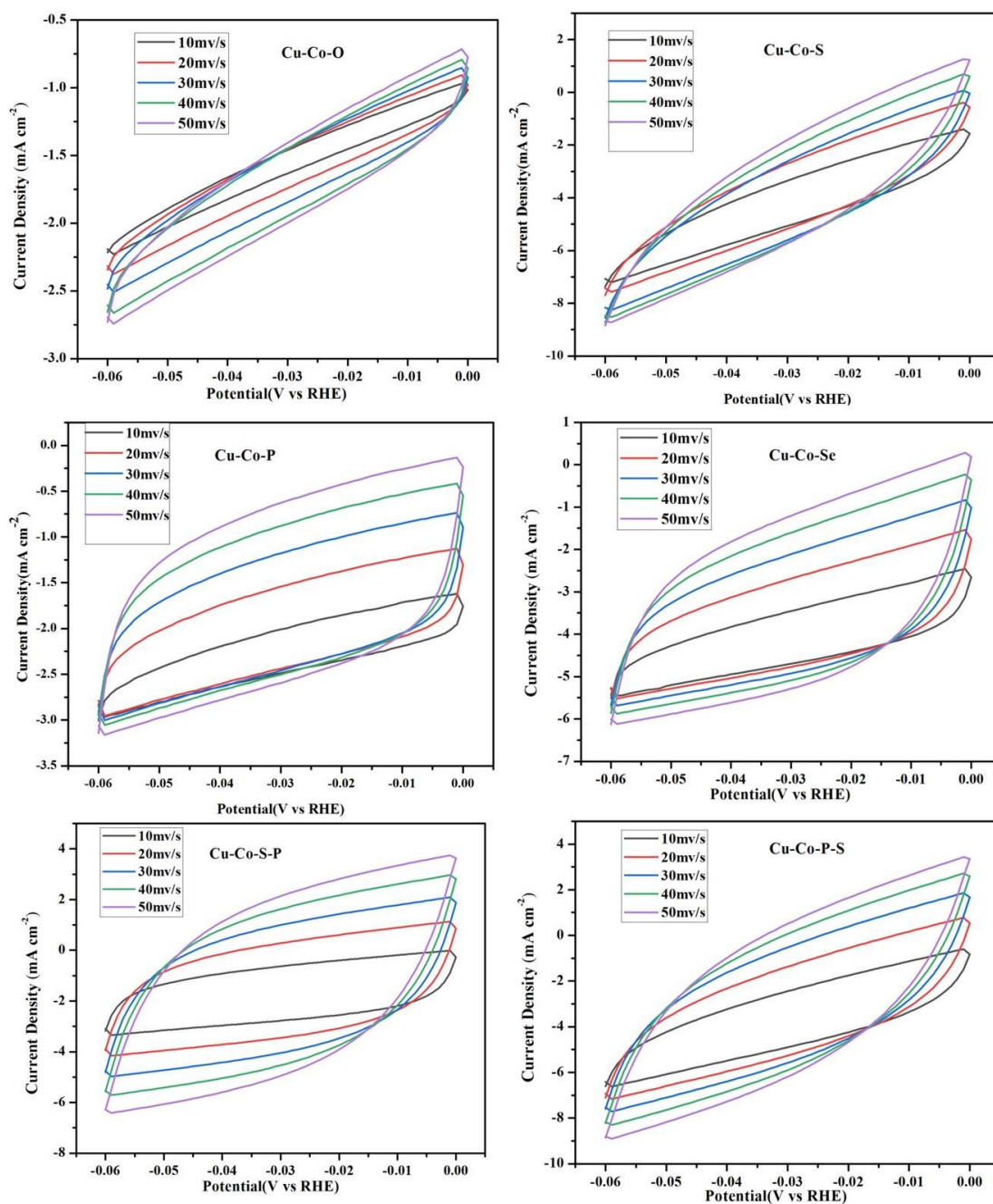


**Fig. S3** CVs of Cu-Co-O, Cu-Co-S, Cu-Co-P, Cu-Co-Se, Cu-Co-S-P and Cu-Co-P-S with different scan rates (10-50 mV s<sup>-1</sup>) in the region of -0.06-0 V vs RHE.

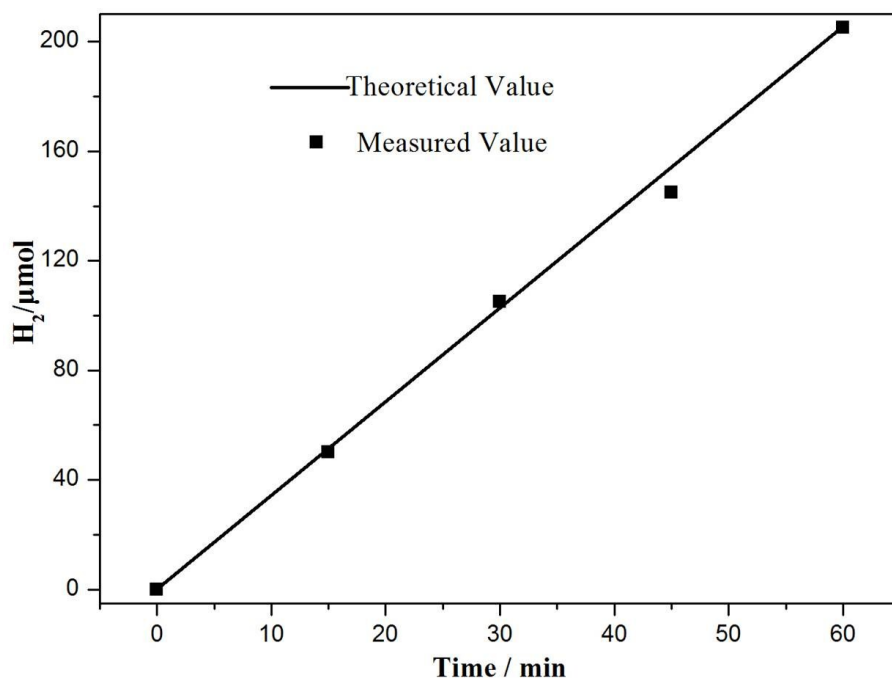


**Fig. S4** Electrocatalytic efficiency of H<sub>2</sub> production over Cu-Co-P-S at a potential of ca. -0.2V, measured for 60 min.

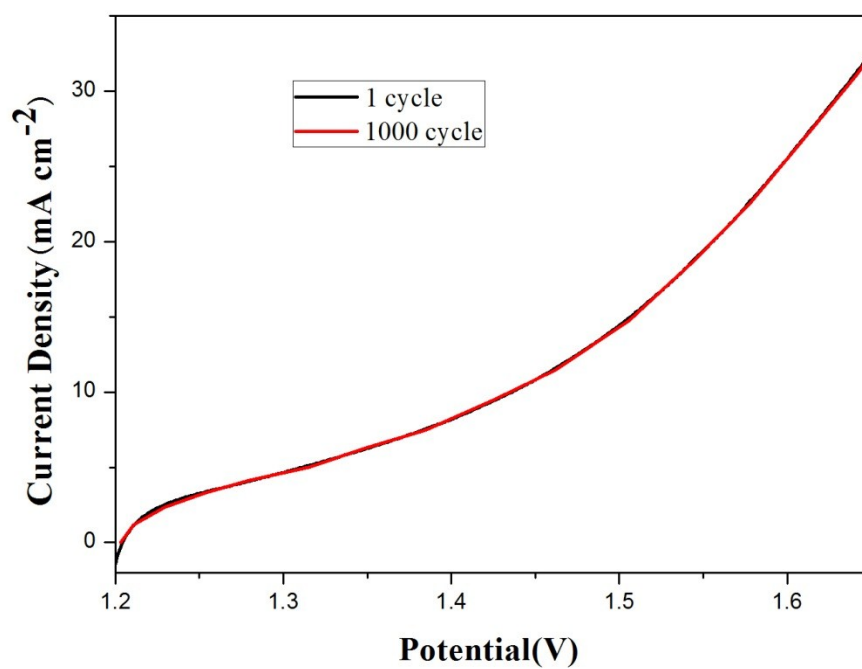


**Fig. S5** The polarization curves for the Cu-Co-P-S before and after 1000 cycles of the accelerated stability test.

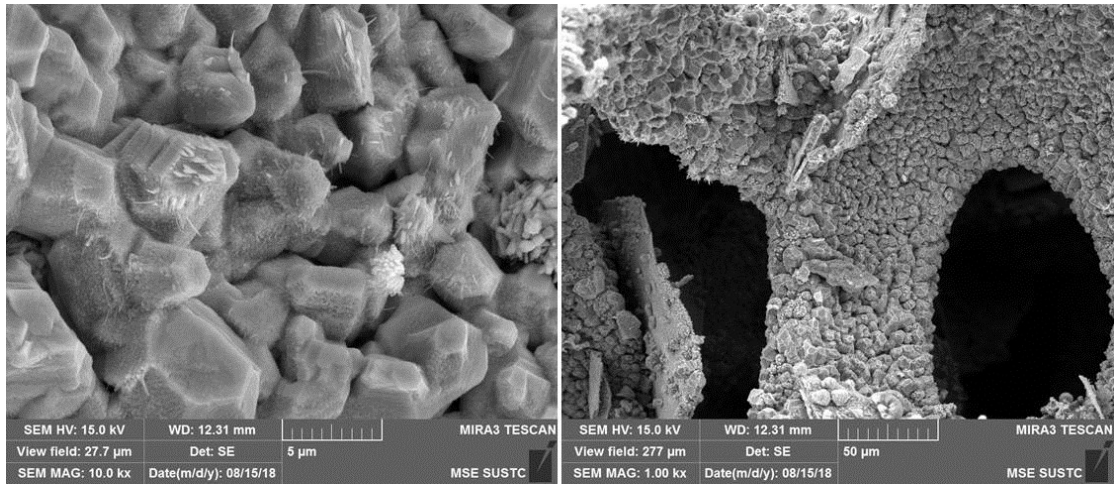


**Fig. S6 SEM of the Cu-Co-S.**

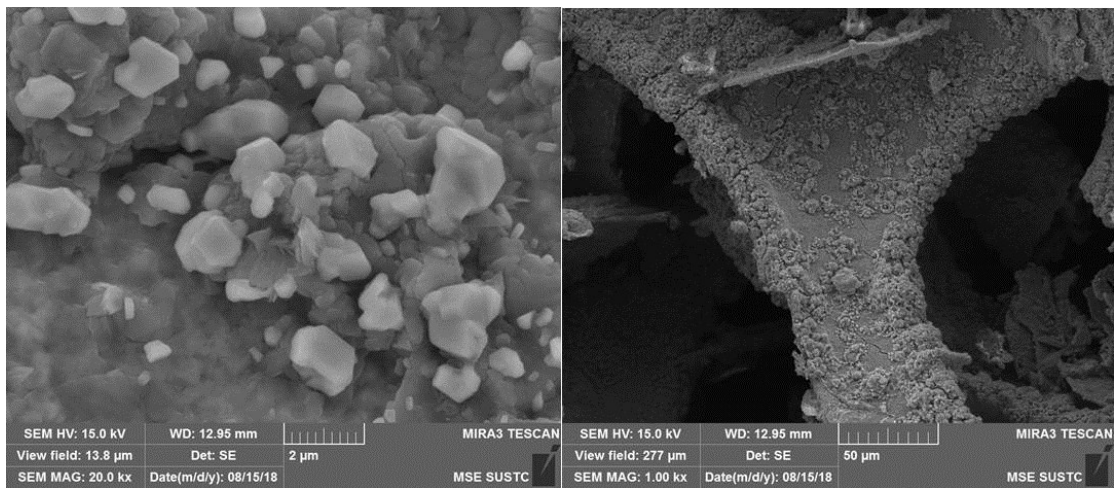


**Fig. S7 SEM of the Cu-Co-P.**

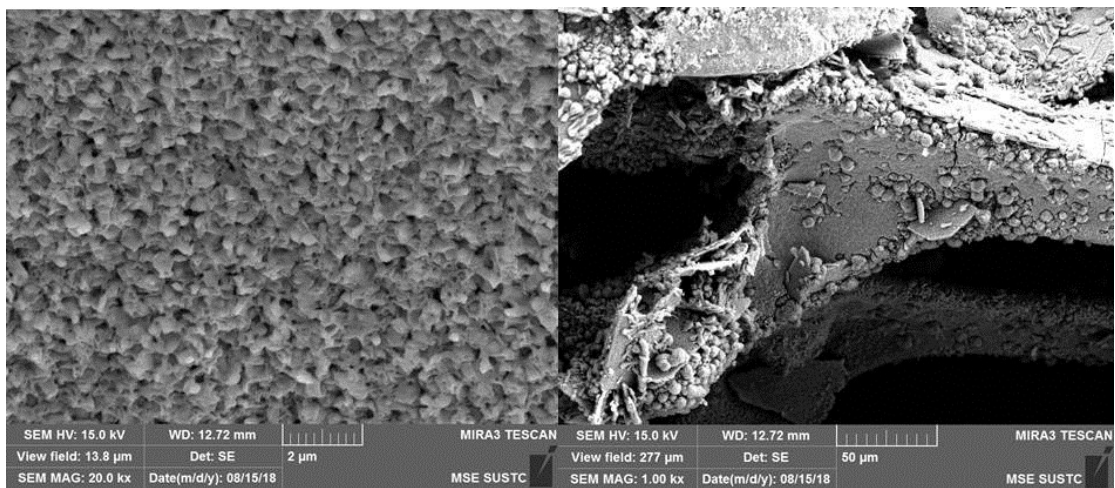


**Fig. S8 SEM of the Cu-Co-Se.**

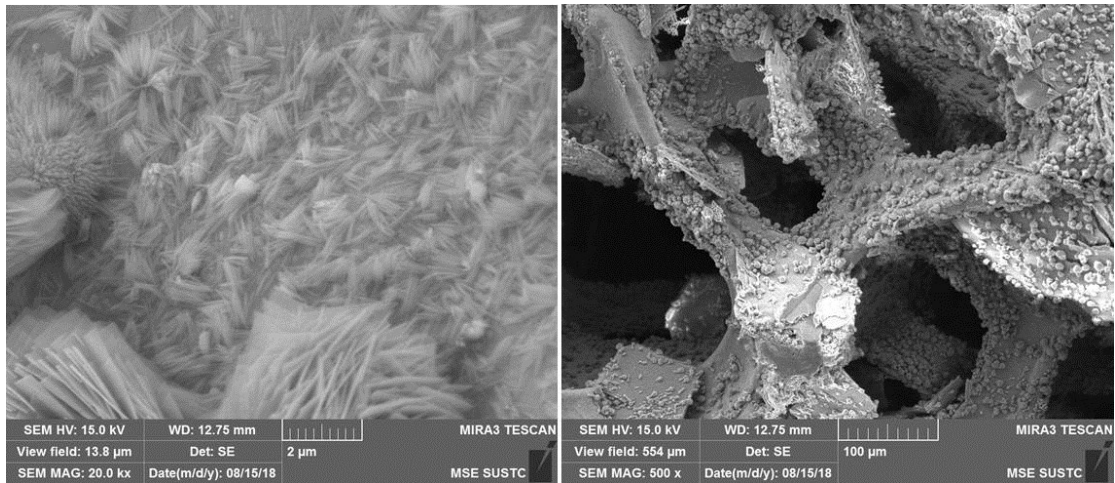


**Fig. S9SEM of the Cu-Co-O.**

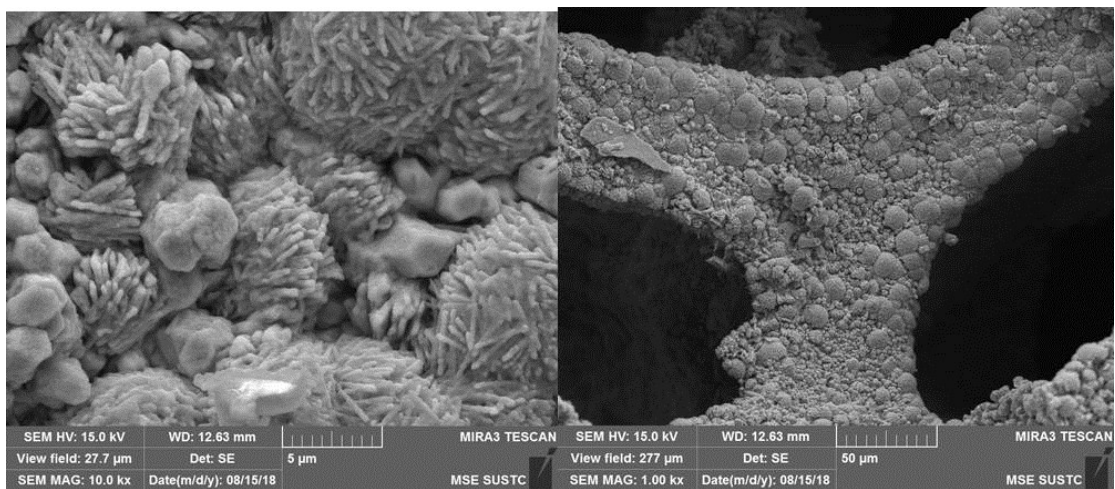


**Fig. S10SEM of the Cu-Co-S-P.**

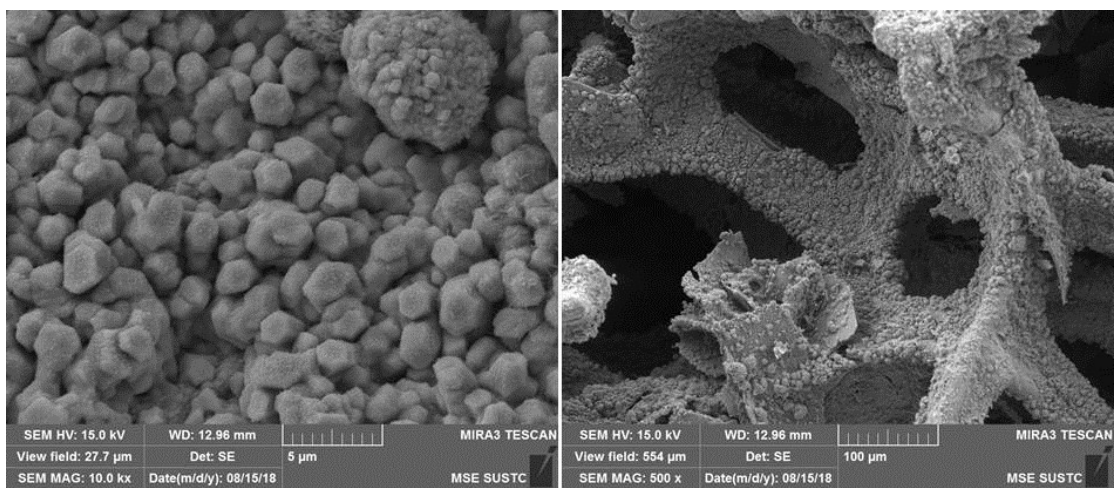


**Fig. S11SEM of the Cu-Co-P-S.**

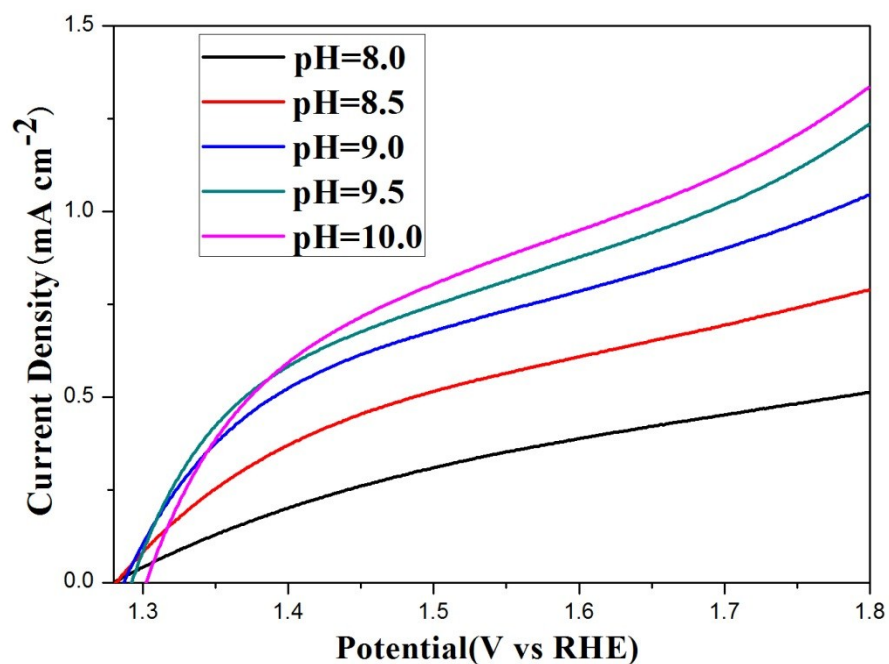


**Fig. S12** LSV of Cu-Co-P-S in 80 mM sodium borate buffer solution at a potential sweep rate of 100 mV s<sup>-1</sup>(1.30-1.80 V vs RHE).

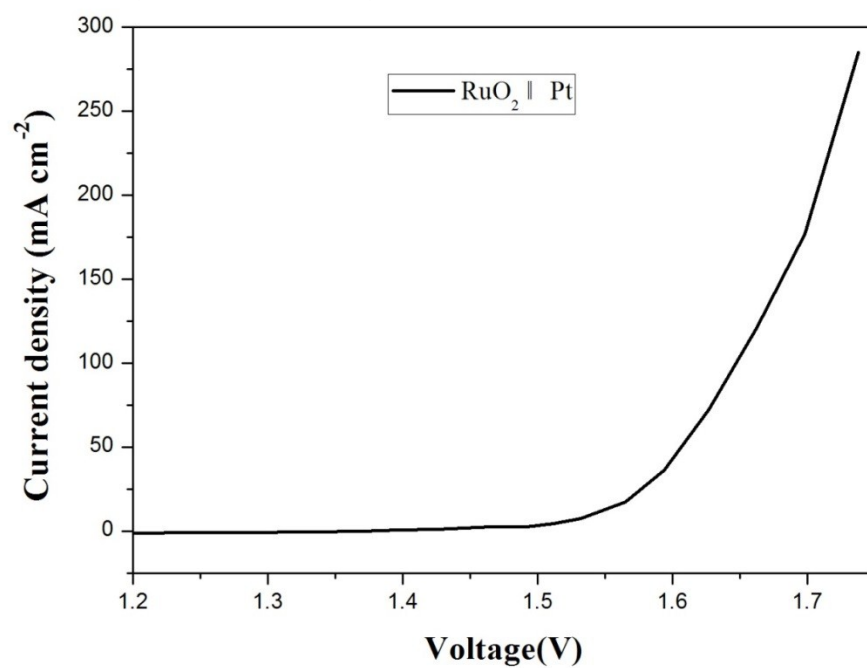


**Fig. S13** Polarization curve of the RuO<sub>2</sub> and Pt for water splitting with a scan rate of 5 mV s<sup>-1</sup> in 1 M KOH.

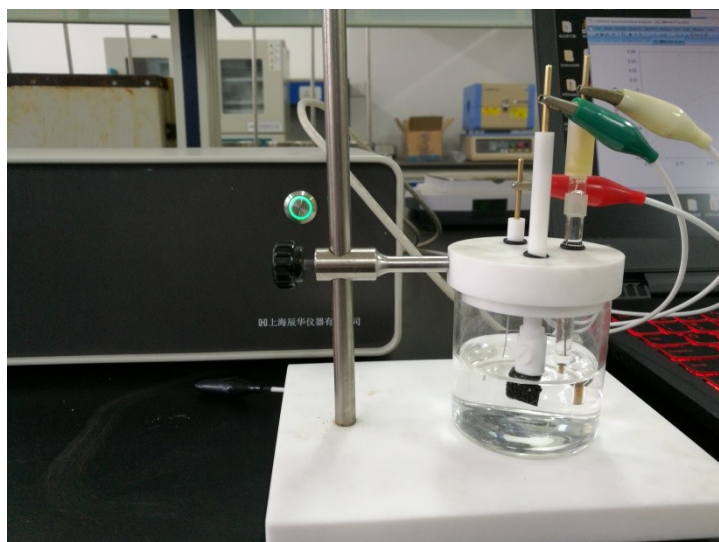


**Fig. S14** A photograph showing generation of O<sub>2</sub> bubbles on the Cu-Co-P-S electrodes.

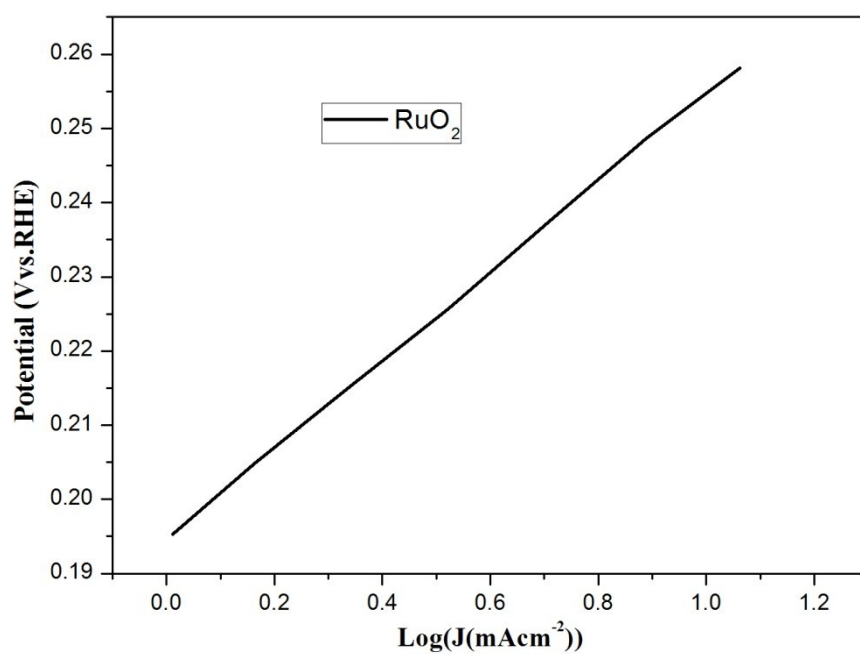


**Fig. S15** Tafel plots of RuO<sub>2</sub> derived from the OER voltammograms.



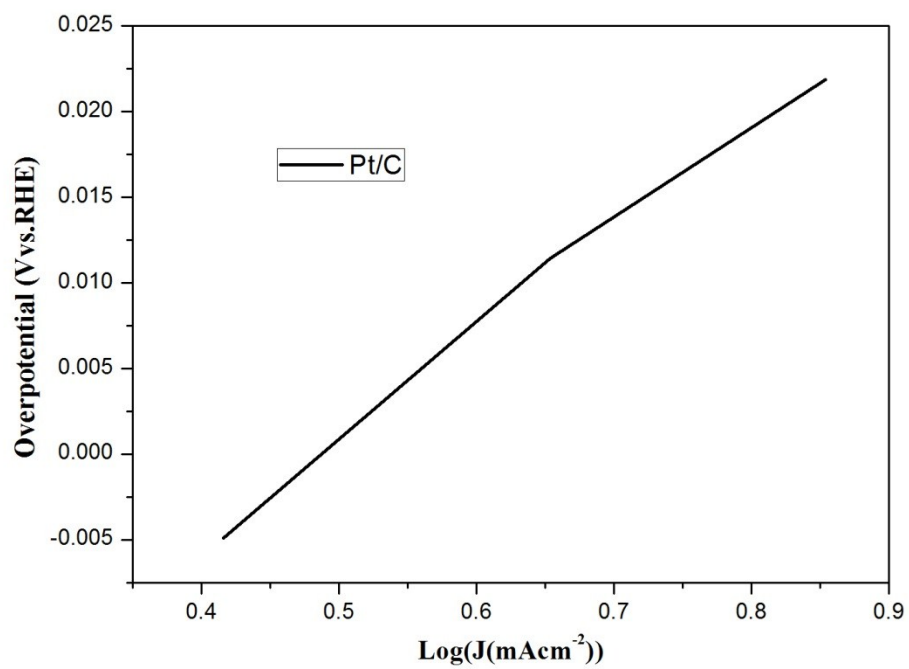


**Fig. S16** Tafel plots of Pt/C derived from the HER voltammograms.

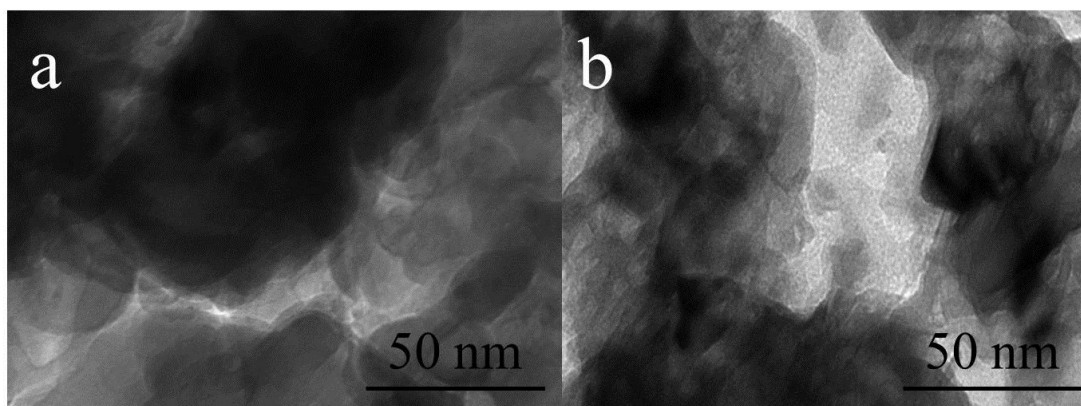


**Fig. S17** TEM of fresh catalyst (a) and recovered catalyst (b).

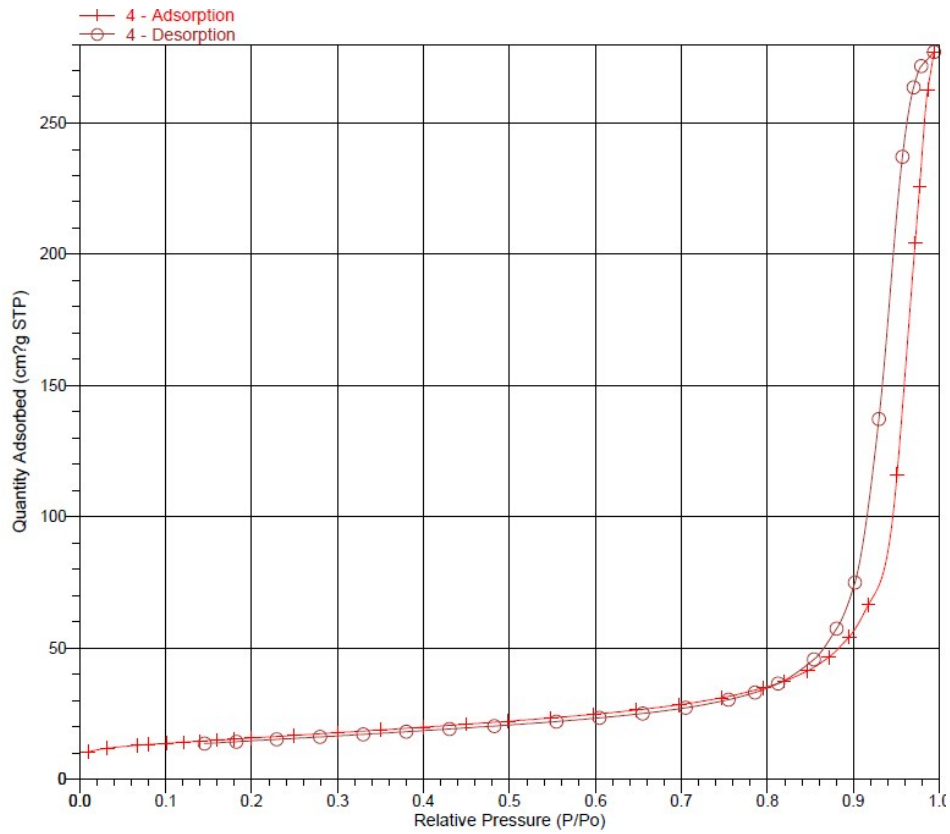


**Fig. S18** Nitrogen adsorption isotherms of the porous Cu-Co-P.

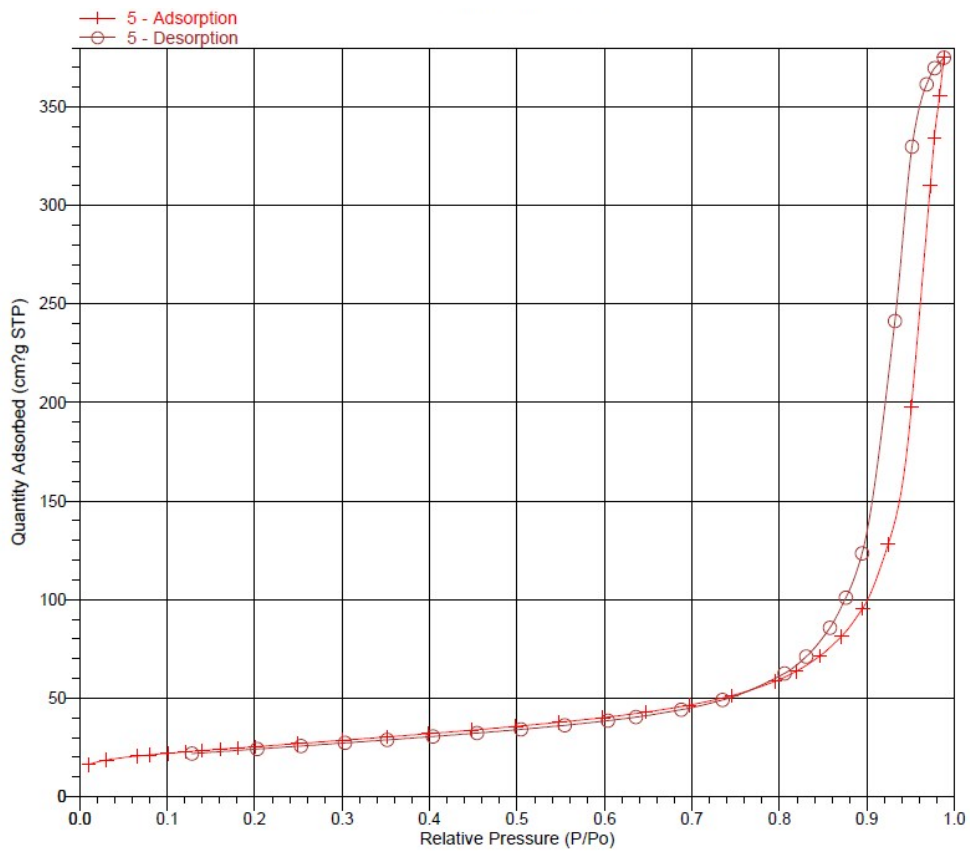


**Fig. S19** Nitrogen adsorption isotherms of the porous Cu-Co-S-P.

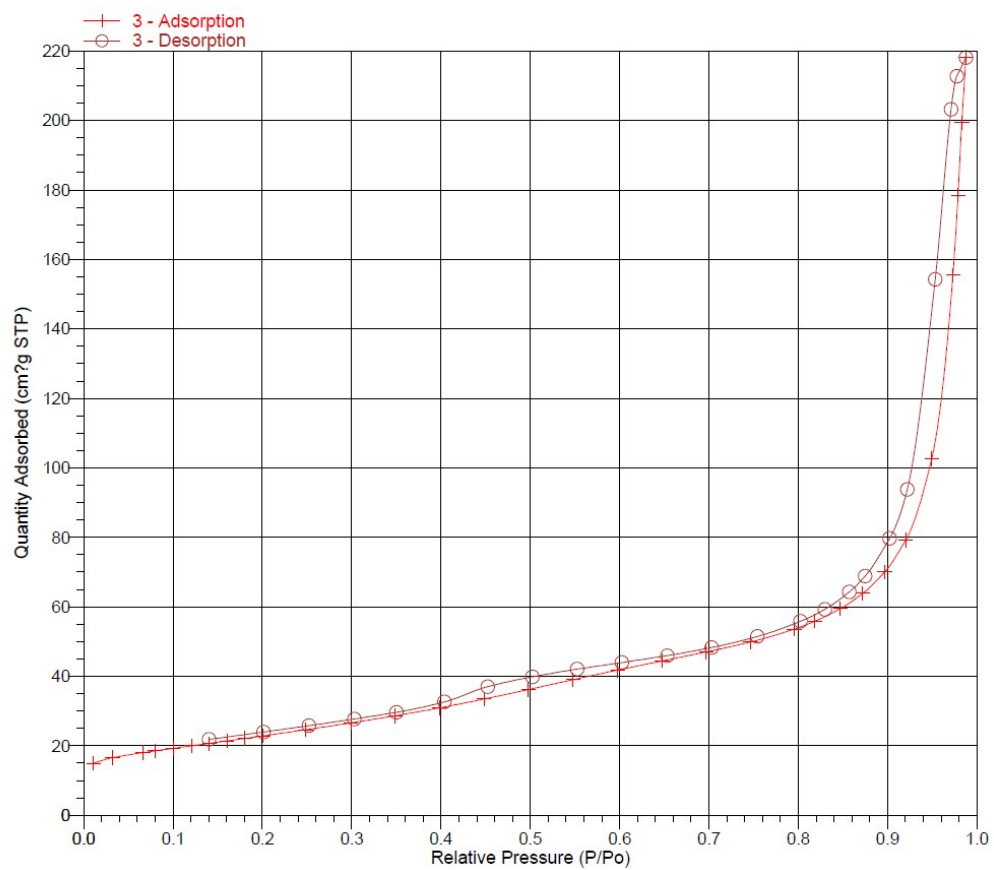


**Fig. S20** Nitrogen adsorption isotherms of the porous Cu-Co-P-S.

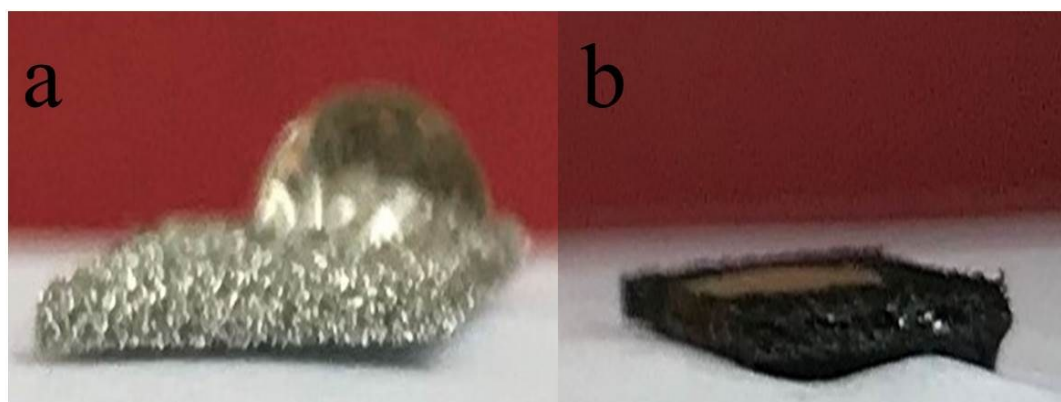


**Fig. S21** Processed digital photos of the hydrophilic property test for pure NF (a) and Cu-Co-P-S (b).

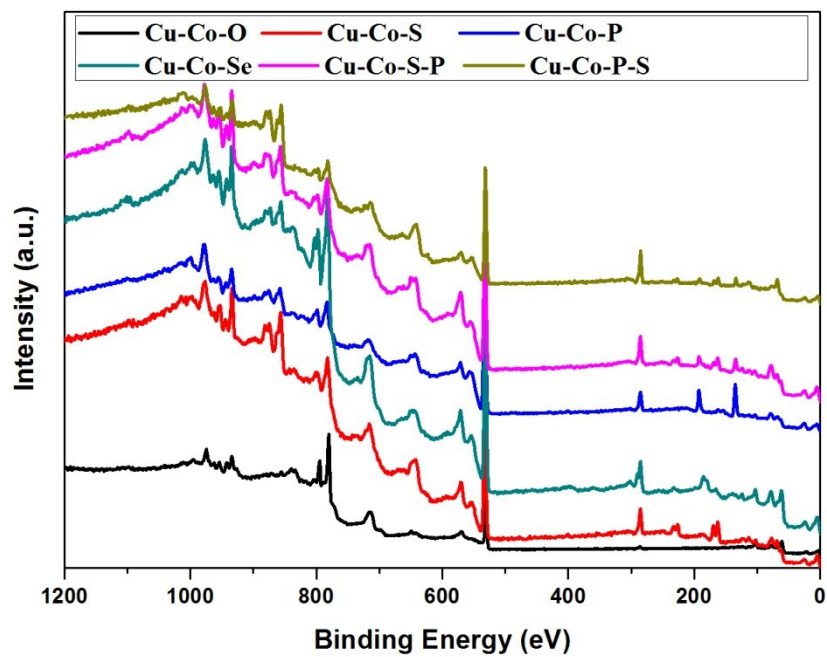


Fig. S22 XPS survey of Cu-Co-O, Cu-Co-S, Cu-Co-P, Cu-Co-Se, Cu-Co-S-P and Cu-Co-P-S.